

Article

Cobalt and Carbon Complex as Counter Electrodes in Dye-Sensitized Solar Cells

Chi-Feng Lin *, Ting-Hsuan Hsieh, Yu-Chen Chou, Pin-Hung Chen, Ci-Wun Chen and Chun-Han Wu

Department of Electro-Optical Engineering, National United University, Miaoli 36063, Taiwan; din5598678@gmail.com (T.-H.H.); byron801202@gmail.com (Y.-C.C.); didi3325s@gmail.com (P.-H.C.); fish616006@gmail.com (C.-W.C.); u0723024@gm.nuu.edu.tw (C.-H.W.)

* Correspondence: chifenglin@nuu.edu.tw

Abstract: We developed cobalt and carbon complex materials as counter electrodes (CEs) for dye-sensitized solar cells (DSSCs) to replace conventional platinum (Pt) CEs. Co12 and Co15, both of which are basic cobalt derivatives, showed good redox potential with a suitable open-circuit voltage (V_{OC}); however, their poor electrical conductivity engendered a low short-circuit current (J_{SC}) and fill factor (FF). Mixing them with carbon black (CB) improved the electrical conductivity of the CE; in particular, J_{SC} and FF were considerably improved. Further improvement was achieved by combining cobalt derivatives and CB through thermal sintering to produce a novel CoCB material as a CE. CoCB had good electrical conductivity and electrocatalytic capability, and this further enhanced both J_{SC} and V_{OC} . The optimized device exhibited a power conversion efficiency (PCE) of 7.44%, which was higher than the value of 7.16% for a device with a conventional Pt CE. The conductivity of CoCB could be further increased by mixing it with PEDOT:PSS, a conducting polymer. The device's J_{SC} increased to 18.65 mA/cm², which was considerably higher than the value of 14.24 mA/cm² for the device with Pt CEs. The results demonstrate the potential of the cobalt and carbon complex as a CE for DSSCs.



Citation: Lin, C.-F.; Hsieh, T.-H.; Chou, Y.-C.; Chen, P.-H.; Chen, C.-W.; Wu, C.-H. Cobalt and Carbon Complex as Counter Electrodes in Dye-Sensitized Solar Cells. *Photonics* **2021**, *8*, 166. <https://doi.org/10.3390/photonics8050166>

Received: 27 March 2021

Accepted: 11 May 2021

Published: 19 May 2021

Publisher's Note: MDPI stays neutral with regard to jurisdictional claims in published maps and institutional affiliations.



Copyright: © 2021 by the authors. Licensee MDPI, Basel, Switzerland. This article is an open access article distributed under the terms and conditions of the Creative Commons Attribution (CC BY) license (<https://creativecommons.org/licenses/by/4.0/>).

Keywords: dye-sensitized solar cells; counter electrodes; cobalt; carbon; conducting polymer

1. Introduction

This paper is an extended version of our paper, Chi-Feng Lin; Pin-Hung Chen; Ting-Hsuan Hsieh; Hsieh-Cheng Han; Kuo-Yuan Chiu: Cobalt derivatives as counter electrodes in dye-sensitized solar cells. In Proceedings of the 2015 22nd International Workshop on Active-Matrix Flatpanel Displays and Devices (AM-FPD), Kyoto, Japan; 1–4 July 2015; Available online: <https://ieeexplore.ieee.org/document/7173248> (accessed on 3 August 2015) [1].

Dye-sensitized solar cells (DSSCs) have attracted considerable research attention in the last two decades. Compared with other types of solar cells, DSSCs afford advantages such as low cost, simple fabrication process, and good conversion efficiency.

DSSCs are mainly composed of three parts: a working electrode (WE), a counter electrode (CE), and an electrolyte. Figure 1 illustrates a schematic and the working principle of a DSSC. First, dye molecules (D) adsorbed on the TiO₂ layer are stimulated to the excited state (D*) by the incident photon energy. Second, the excited dye molecules (D*) transfer electrons to the TiO₂ layer and external circuit, and thus reach an oxidized state (D⁺). Third, the dye molecules (D⁺) in the oxidized state return to the ground state (D) by accepting electrons from the iodide ion (I[−]) in the electrolyte; thus, I[−] changes into I₃[−] [2]. Finally, I₃[−] changes back into I[−] by accepting electrons from the external circuit through the CE.

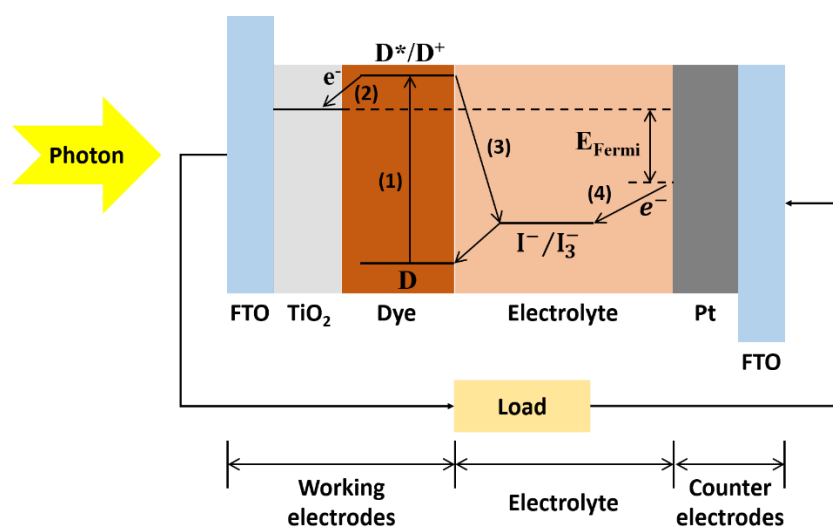


Figure 1. Schematic and working principle of DSSCs.

Electrolyte and CEs play the key roles of catalytic reduction and electron conduction in DSSCs. Developments of electrolyte in recent years are mostly focus on cobalt-based electrolyte, water-based, and polymer-based systems [3–8]. For the CEs parts, platinum (Pt) is used most commonly as a CE material. In 1991, Grätzel first used a Pt CE and reported a conversion efficiency of 7.1%, which was derived from the high conductivity, chemical stability, and excellent catalytic reduction ability of the CE [9,10].

Although Pt shows excellent catalytic reduction ability, it is an expensive metal; therefore, its use increases the cost of DSSCs. Accordingly, studies have attempted to reduce costs and to find suitable substitutes for Pt. Specifically, studies have investigated the use of other composite materials [5], such as carbon materials [11–21], titanium nitride [22,23], conducting polymer [24–26], cobalt (Co) composites [27], and cobalt sulfide [28–36], as CEs to replace Pt. Among these, cobalt composite materials have good electrochemical properties and low cost, and they are abundantly available [37–40]. Cobalt composites and related structures, when used as CEs, show high photoelectric conversion efficiency [41–43], making them a popular substitute for Pt in recent years [44–48].

In this study, we used various types of cobalt derivatives, including commercialized materials such as cobalt(II) acetate tetrahydrate and vitamin B12 (VB12), as well as the newly designed cobalt derivatives Co12 and Co15, as CEs in DSSCs. Furthermore, we combined cobalt derivatives and carbon black (CB) to produce new complex materials. Consequently, devices with Co12+CB and Co15+CB CEs showed power conversion efficiency (PCE) levels of 5.46% and 6.74%, respectively. These values are close to the aforementioned PCE of 7.16% for a device with PT CEs. Furthermore, we combined VB12 and CB through thermal sintering to produce a novel CoCB material as a CE. We also improved the conductivity of CoCB with a conducting polymer. The optimized device showed a PCE of 7.44%, which is higher than those of the aforementioned devices. Therefore, this result indicated that the cobalt complex could be used as a substitute CE material in DSSCs.

2. Materials and Methods

DSSCs consist of a WE, an electrolyte, and a CE. To fabricate WEs, we first dissolved polyethylene glycol, anhydrous titanium oxide powder (P25, ACROS ORGANIS), and titanium isopropoxide in ethanol to produce a TiO₂ slurry. Then, we spin-coated this slurry on fluorine-doped tin oxide (FTO) substrates with an area of 0.24 cm². After the spin coating process, the TiO₂ films were annealed in the furnace under 450 °C for one hour to obtain the porous TiO₂ layer. Finally, the TiO₂ electrodes were immersed in N719 dye (UR-N719, Solaronix) for 12 h to obtain the WEs.

Conventional Pt CEs were fabricated through the thermal cracking process: 20 μL hexachloroplatinic acid at concentration of 0.2 M was titrated on the FTO substrates and then baked under 80 $^{\circ}\text{C}$ to remove solvent. After the titration process, Pt films were annealed under 390 $^{\circ}\text{C}$ for 15 min to obtain Pt CEs. All cobalt complexes (cobalt(II) acetate tetrahydrate, VB12, Co12, Co15, and CoCB) were dissolved in 1 M tetrahydrofuran (THF). Subsequently, the solution was spin-coated on the FTO substrate and baked to form a thin film for CEs. Finally, we assembled the WEs and CEs together and injected the iodine-based electrolyte with LiI, I_2 , and TBP at the concentration of 0.5, 0.05, and 0.5 M, respectively. After device fabrication, current–voltage (J–V) characteristics were measured using an I–V sourcemeter (Keithley 2400) under the illumination of a 1-sun AM 1.5G solar simulator that was calibrated using a Si reference cell. The optical properties of the CEs were measured using ultraviolet (UV)-visible spectroscopy (UV-3101PC, SHIMADZU).

All experiments were repeated at least three times to make sure of the reproducibility of the device and phenomena and to ensure the run-to-run variation for the same experiment was within 5%. Besides, at least six devices were prepared for each parameter in every experiment to confirm the stability of the fabrication process and the standard deviation of each performance of the devices were calculated to show the stability.

3. Results and Discussion

Figure 2 presents the transmittance spectra of various CEs and their photographs. The spectrum of each material is the average result of six samples in one experiment, and the experiment is performed 3 times with different samples and the run-to-run variation is within 5%. All the substitute CE materials, especially the cobalt derivatives, showed high transparency in the wavelength range of 400–800 nm. The high transparency of CEs may be a drawback relative to Pt CEs because less light will be reflected back to the devices, thereby decreasing the absorption of WEs and in turn reducing the photocurrent and device efficiency. Nevertheless, the high transparency of the electrodes demonstrates their potential for use in devices for transparent electronics and building-integrated photovoltaic (BIPV) applications [49].

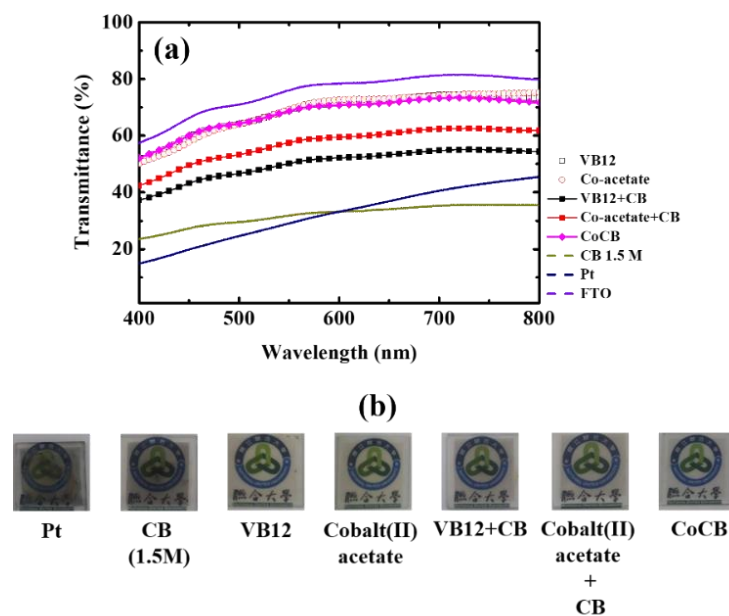


Figure 2. (a) Transmittance spectra and (b) photographs of various CEs.

Figure 3 shows the J–V characteristics of the DSSCs with cobalt derivatives as CEs, and Table 1 lists the device performance levels. The results for each CE are the average values of six devices in one experiment, and the standard deviation of the device performance levels was calculated from the data of five devices in one experiment. The experiment was

repeated at least 3 times and the run-to-run variation was within 5%. The performance levels of the devices with the cobalt derivative CEs were considerably higher than those of the devices with the FTO CEs, although the PCE was still much lower than the device with Pt CE. It is well-known that FTO is not the appropriate catalytic material for CEs owing to its low oxidation-reduction potential and poor electrocatalytic capability. Comparing the device with FTO CE, devices with the VB12 and cobalt(II) acetate CEs showed a V_{OC} of more than 0.7 V. The device with cobalt(II) acetate CEs even showed 0.85 V in V_{OC} , much higher than that with Pt CE, indicating the good oxidation-reduction potential of cobalt(II) acetate for CE application in DSSC. All devices with the cobalt series CEs showed a good open-circuit voltage (V_{OC}) but poor short-circuit current (J_{SC}) and fill factor (FF), resulting in low PCE. The results showed that cobalt derivatives have good oxidation-reduction potential but overly low conductivity, resulting in a high series resistance and large charge recombination in the device.

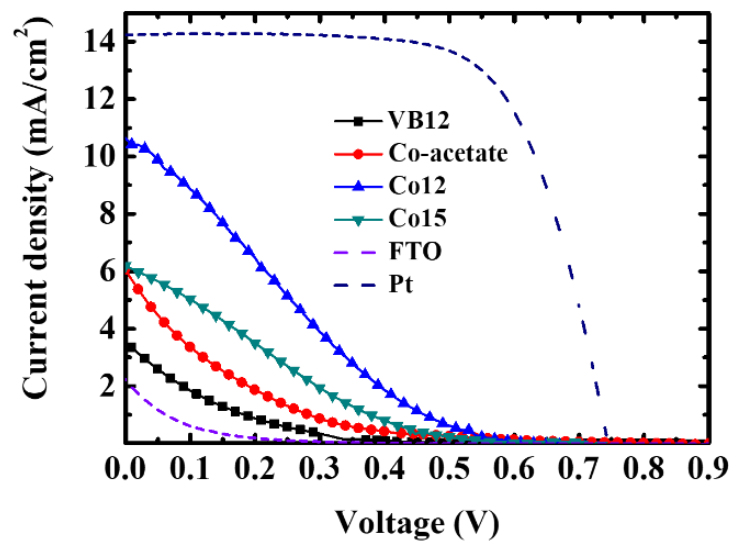


Figure 3. J–V characteristics of DSSCs with various cobalt derivatives as CEs.

Table 1. Performance levels of DSSCs with various cobalt derivatives as CEs. The values in the brackets are the standard deviation.

CEs	J_{SC} (mA/cm ²)	V_{OC} (V)	FF	η (%)
VB12	3.34 (0.59)	0.71 (0.01)	8.17 (1.08)	0.19 (0.01)
Cobalt(II) acetate	5.71 (0.22)	0.85 (0.01)	8.08 (1.02)	0.38 (0.02)
Co12	10.59 (0.57)	0.62 (0.01)	19.84 (1.01)	1.25 (0.11)
Co15	6.08 (0.21)	0.63 (0.01)	18.37 (1.23)	0.70 (0.27)
Pt	14.24 (0.29)	0.75 (0.02)	67.12 (0.26)	7.16 (0.09)
FTO	2.21 (0.28)	0.44 (0.01)	6.73 (0.61)	0.06 (0.01)

To increase the conductivity of the materials, new cobalt derivatives, Co12 and Co15, were synthesized. These devices showed increased J_{SC} values compared with the VB12 and cobalt(II) acetate CEs. The device with the Co12 CEs showed a J_{SC} value of more than 10 mA/cm² and FF close to 20, resulting in a PCE of more than 1%, which is three times higher than that of the commercialized cobalt derivatives used as CEs. The PCE

remained low, indicating that the CEs of the devices could be optimized by enhancing the conductivity of cobalt derivatives.

To increase the conductivity of cobalt derivatives, we introduced CB. This is because carbon materials afford high conductivity, catalytic activities, and surface area, and are thus good candidates for replacing Pt as CEs. CB, in addition to possessing the advantages of carbon materials, is inexpensive and is thus considered a good CE for DSSCs. CB was dissolved in 1.5 M THF and then mixed with a solution of cobalt derivatives at the same volume ratio. For comparison, devices with pure CB CE at CB concentrations of 0.75 and 1.5 M were also prepared. Figure 4 illustrates the J–V characteristics of DSSCs with cobalt derivatives mixed with CB as CEs, and Table 2 lists the device performance levels. In particular, J_{SC} and FF were found to be significantly enhanced, resulting in a large improvement in the PCE of the devices with cobalt derivatives and CB as CEs. The J_{SC} value of the device with the Co15+CB CE increased from 6.08 to 11.15 mA/cm² (i.e., an 83% improvement) compared with that of the device with the Co15 CE. Furthermore, the FF of the devices with Co12+CB and Co15+CB CEs was improved by more than three times, which is a similar improvement to that achieved with the use of conventional Pt CEs. However, the device with the pure CB CE showed higher V_{OC} , J_{SC} , and PCE values than did the device with the Co+CB CE, indicating that the enhanced device performance may be attributed to the contribution of the CB alone. Specifically, the introduction of cobalt derivatives reduced the electrical properties and electrocatalytic capability of CB. Nevertheless, it should be noticed that compared with pure CB solution at a concentration of 1.5 M, there was only half the amount of CB in the Co+CB mixed solution. It can be found that the J_{SC} of the device with 0.75 M CB as CE is lower than the device with Co12+CB as CE. It indicates that the improvement of the device was not only contributed by CB, but the interaction between Co12 and CB further increased the conductivity of CE after replacing half the amount of CB with Co12. Besides, the FF of the device with the Co15+CB CE was higher than that of the device with the CB CE, and the improvements in the performance and efficiency of the device with the Co15+CB CE were higher than those of the device with the Co12+CB. This trend was opposite to that of pure cobalt derivative CEs, indicating that the cobalt derivatives were modified by CB.

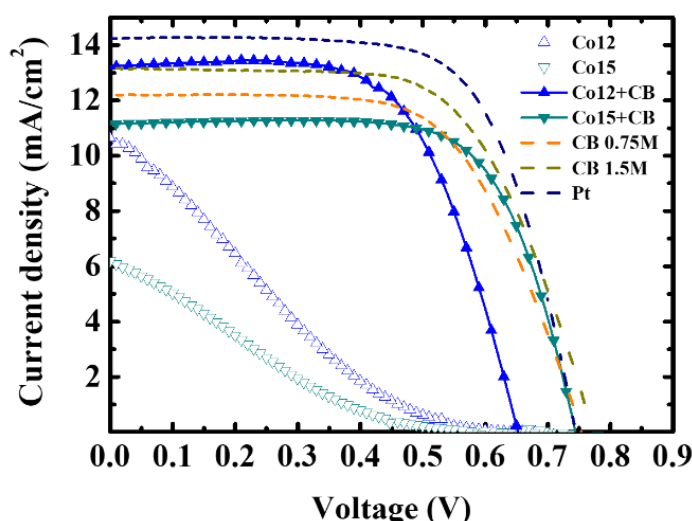


Figure 4. J–V characteristics of DSSCs with cobalt derivatives mixed with CB as CEs.

Table 2. Performance levels of DSSCs with cobalt derivatives mixed with CB as CEs. The values in the brackets are the standard deviation.

CEs	J _{sc} (mA/cm ²)	V _{oc} (V)	FF	η (%)
Co12	10.59 (0.57)	0.62 (0.01)	19.84 (1.01)	1.25 (0.11)
Co12+CB	13.23 (0.14)	0.65 (0.01)	63.28 (2.08)	5.42 (0.26)
Co15	6.08 (0.21)	0.63 (0.01)	18.37 (1.23)	0.70 (0.27)
Co15+CB	11.15 (0.33)	0.74 (0.01)	65.46 (1.73)	5.81 (0.19)
CB (1.5 M)	13.17 (0.08)	0.77 (0.01)	63.92 (1.05)	6.38 (0.08)
CB (0.75 M)	12.21 (0.09)	0.75 (0.01)	63.28 (1.13)	5.76 (0.1)
Pt	14.24 (0.29)	0.75 (0.01)	67.12 (0.26)	7.16 (0.09)

To further improve the electrical properties and electrocatalytic capability of cobalt derivatives, we combined VB12 and CB through thermal sintering to produce a novel CoCB material. We also improved the conductivity of CoCB with the conducting polymer poly(3,4-thylenedioxythiophene):poly(styrenesulfonate) (PEDOT:PSS). Figure 5 presents the J–V characteristics of the DSSCs with CoCB modified with PEDOT:PSS as CEs, and Table 3 lists the device performance levels. The device with pure PEDOT:PSS as CE was also prepared for comparison. The results indicated that both the conductivity and the redox ability of VB12 were greatly improved by CB. The device with the CoCB CE showed a J_{SC} value of 13.75 mA/cm², V_{OC} value of 0.78 V, and FF of 69.28, all of which were higher than the corresponding parameters of the device with the CB CE. The V_{OC} and FF of the device with the CoCB CE were even higher than those of the device with the Pt CE, and they considerably improved the PCE of the device. The optimized device with the CoCB CE showed a PCE of 7.44%, and this value is higher than those of devices with both CB and Pt CEs.

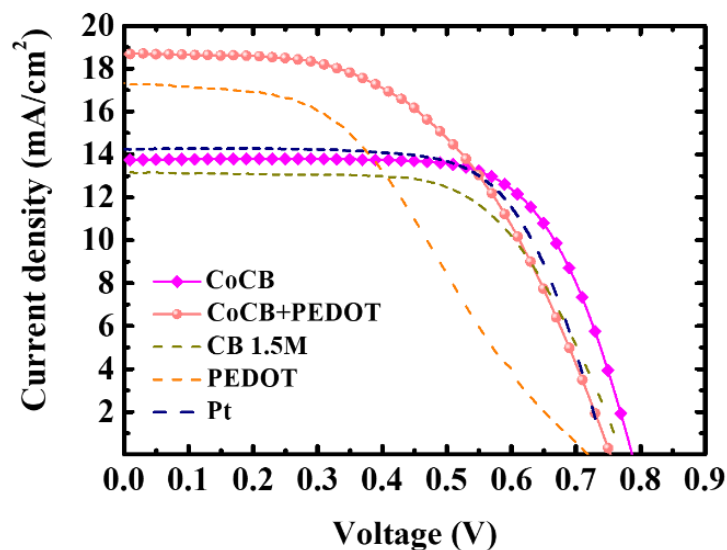


Figure 5. J–V characteristics of DSSCs with series of cobalt complex CEs.

Table 3. Performance levels of DSSCs with cobalt complex CEs. The values in the brackets are the standard deviation.

CEs	J _{SC} (mA/cm ²)	V _{OC} (V)	FF	η (%)
CoCB	13.75 (0.29)	0.78 (0.02)	69.28 (0.45)	7.44 (0.22)
CoCB +	18.65 (0.63)	0.75 (0.02)	51.31 (1.49)	7.13 (0.18)
PEDOT:PSS	13.17 (0.08)	0.77 (0.01)	63.92 (1.05)	6.38 (0.08)
CB (1.5M)	17.33 (0.42)	0.72 (0.02)	42.60 (2.13)	5.32 (0.38)
PEDOT:PSS	14.24 (0.29)	0.75 (0.01)	67.12 (0.26)	7.16 (0.09)
Pt				

We also attempted to further improve the conductivity of CoCB by mixing the CoCB solution with PEDOT:PSS. The device with pure PEDOT:PSS CE showed higher J_{SC} compared with all other devices because of the high conductivity, but the low electrocatalytic capability of PEDOT:PSS increased recombination of the carrier and thus reduced FF of the device. After mixing CoCB with PEDOT:PSS, as shown in Figure 5 and Table 3, J_{SC} increased from 13.75 to 18.65 mA/cm², which was higher than the J_{SC} of 14.24 mA/cm² for the device with the Pt CE. However, the lower redox ability of PEDOT:PSS reduced the V_{OC} and FF, resulting in the device having a slightly lower PCE of 7.13%.

4. Conclusions

This study investigated the use of a series of cobalt derivatives as CEs to replace conventional Pt CEs in DSSCs. Co12 and Co15, both of which are basic cobalt derivatives, showed suitable J_{SC} and V_{OC} values for application as CEs; however, they had low FF owing to their poor conductivity and redox ability. After Co12 and Co15 were mixed with CB, the device performance was obviously enhanced. Further improvement was achieved by combining conventional VB12 and CB through thermal sintering to form a novel CoCB material as a CE. The J_{SC} and V_{OC} values were improved owing to the good conductivity and redox ability of CoCB, and the optimized device showed a PCE of 7.44%, which was higher than that of the control device with conventional Pt CEs. The conductivity of CoCB could be further increased by mixing CoCB with PEDOT:PSS. The high conductivity of PEDOT:PSS contributed to a further increase in J_{SC}; however, its lower redox ability reduced the V_{OC} and FF. The results demonstrate the potential of the cobalt and carbon complex as a CE for DSSCs.

Author Contributions: Conceptualization, C.-F.L.; Data curation, T.-H.H., Y.-C.C., P.-H.C., C.-W.C. and C.-H.W.; Investigation, T.-H.H., Y.-C.C., P.-H.C. and C.-W.C.; Supervision, C.-F.L.; Writing—original draft, C.-F.L., Y.-C.C. and C.-H.W.; Writing—review & editing, C.-F.L. All authors have read and agreed to the published version of the manuscript.

Funding: This research was funded by the Ministry of Science and Technology, R.O.C., under grant numbers MOST 105-2221-E-239-024, 106-2221-E-239-020, 107-2221-E-239-020-MY2, and 109-2221-E-239-030.

Conflicts of Interest: The authors declare no conflict of interest.

References

- Lin, C.F.; Chen, P.H.; Hsieh, T.H.; Han, H.C.; Chiu, K.Y. Cobalt derivatives as counter electrodes in dye sensitized solar cells. In Proceedings of the 2015 22nd International Workshop on Active-Matrix Flatpanel Displays and Devices (AM-FPD), Kyoto, Japan, 1–4 July 2015.
- Popov, A.I.; Geske, D.H. Studies on the Chemistry of Halogen and of Polyhalides. XIII. Voltammetry of Iodine Species in Acetonitrile. *J. Am. Chem. Soc.* **1958**, *80*, 1340–1352. [[CrossRef](#)]

3. Imperiyka, M.; Ahmad, A.; Hanifah, S.A.; Bella, F. A UV-prepared linear polymer electrolyte membrane for dye-sensitized solar cells. *J. Phys. B* **2014**, *450*, 151–154. [[CrossRef](#)]
4. Sacco, A.; Bella, F.; Pierre, S.D.L.; Cstellino, M.; Bianco, S.; Bongiovanni, R.; Pirri, C.F. Electrodes/Electrolyte Interfaces in the Presence of a Surface-Modified Photopolymer Electrolyte: Application in Dye-Sensitized Solar Cells. *Chem. Phys. Chem.* **2015**, *16*, 960–969. [[CrossRef](#)] [[PubMed](#)]
5. Mariotti, N.; Bonomo, M.; Fagiolari, L.; Barbero, N.; Gerbaldi, C.; Bella, F.; Barolo, C. Recent advances in eco-friendly and cost-effective materials towards sustainable dye-sensitized solar cells. *Green Chem.* **2020**, *22*, 7168–7218. [[CrossRef](#)]
6. Galliano, S.; Bella, F.; Bonomo, M.; Viscardi, G.; Gerbaldi, C.; Boschloo, G.; Barolo, C. Hydrogel Electrolytes Based on Xanthan Gum: Green Route towards Stable Dye-Sensitized Solar Cells. *Nanomaterials* **2020**, *10*, 1585. [[CrossRef](#)]
7. Devadiga, D.; Selvakumar, M.; Shetty, P.; Mahesha, M.G.; Devadiga, M.G.; Devadiga, D.; Ahipa, T.N.; Kumar, S.S. Novel photosensitizer for dye-sensitized solar cell based on ionic liquid-doped blend polymer electrolyte. *J. Solid State Electrochem.* **2021**, *25*, 1461–1478. [[CrossRef](#)]
8. Wu, Z.S.; Zhang, J.; Guo, W.J.; Liu, Y.D.; Wan, D.Y.; Long, J.X.; Cheng, Z.J. Effects of side substituents in bithiophene spacer on the performance of dye-sensitized solar cells with cobalt electrolyte. *Sol. Energy* **2021**, *218*, 503–511. [[CrossRef](#)]
9. Fang, X.M.; Ma, T.L.; Guan, G.Q.; Akiyama, M.; Kida, T.; Abe, E. Effect of the thickness of the Pt film coated on a counter electrode on the performance of a dye-sensitized solar cell. *J. Am. Chem. Soc.* **2004**, *570*, 257–263. [[CrossRef](#)]
10. O'Regan, B.; Grätzel, M. A low-cost, high-efficiency solar cell based on dye-sensitized colloidal TiO₂ films. *Nature* **1991**, *335*, 737–740. [[CrossRef](#)]
11. Yue, G.T.; Wu, J.H.; Xiao, Y.M.; Lin, J.M.; Huang, M.L. Lowcost poly(3,4-ethylenedioxythiophene):polystyrenesulfonate/carbon black counter electrode for dye-sensitized solar cells. *Electrochim. Acta.* **2012**, *67*, 113–118. [[CrossRef](#)]
12. Huang, Z.; Liu, X.Z.; Li, K.X.; Li, D.M.; Luo, Y.H.; Li, H.; Song, W.B.; Chen, L.Q.; Meng, Q.B. Application of carbon materials as counter electrodes of dye-sensitized solar cells. *Electrochem. Commun.* **2007**, *9*, 596–598. [[CrossRef](#)]
13. Suzuki, K.; Yamaguchi, M.; Kumagai, M.; Yanagida, S. Application of Carbon Nanotubes to Counter Electrodes of Dye-sensitized Solar Cells. *Chem. Lett.* **2003**, *32*, 28–29. [[CrossRef](#)]
14. Liu, Z.; Tabakman, S.; Welsher, K.; Dai, H.J. Carbon Nanotubes in Biology and Medicine: In vitro and in vivo Detection, Imaging and Drug Delivery. *Nano Res.* **2009**, *2*, 85–120. [[CrossRef](#)]
15. Li, P.J.; Wu, J.H.; Lin, J.M.; Huang, M.L.; Huang, Y.F.; Li, Q.H. High-performance and low platinum loading Pt/Carbon black counter electrode for dye-sensitized solar cells. *Sol. Energy J.* **2009**, *83*, 845–849. [[CrossRef](#)]
16. Deng, M.H.; Zhang, Q.X.; Huang, S.Q.; Li, D.M.; Luo, Y.H.; Shen, Q.; Toyoda, T.; Meng, Q. Low-Cost Flexible Nano-Sulfide/Carbon Composite Counter Electrode for Quantum-Dot-Sensitized Solar Cell. *Nanoscale Res. Lett.* **2010**, *5*, 986–990. [[CrossRef](#)] [[PubMed](#)]
17. Gao, Z.Y.; Liu, N.; Wu, D.; Tao, W.U.; Xu, F.; Jiang, K. Graphene–CdS composite, synthesis and enhanced photocatalytic activity. *Appl. Surf. Sci.* **2012**, *258*, 2473–2478. [[CrossRef](#)]
18. Yue, G.T.; Wu, J.H.; Xiao, Y.M.; Lina, J.M.; Huang, M.L.; Lan, Z.; Fana, L. Functionalized graphene/poly(3,4-ethylenedioxythiophene):polystyrenesulfonate as counter electrode catalyst for dye-sensitized solar cells. *Energy J.* **2013**, *54*, 315–321. [[CrossRef](#)]
19. Lin, C.F.; Chou, Y.C.; Haung, J.F.; Chen, P.H.; Han, H.C.; Chiu, K.Y.; Su, Y.O. Dye sensitized solar cells with carbon black as counter electrodes. *Jpn. J. Appl. Phys.* **2016**, *55*, 03CE01-4. [[CrossRef](#)]
20. Vijaya, S.; Landi, G.; Wu, J.J.; Anandan, S. MoS₂ nanosheets based counter electrodes: An alternative for Pt-free dye-sensitized solar cells. *Electrochim. Acta* **2019**, *294*, 134–141. [[CrossRef](#)]
21. Jiang, Q.S.; Chen, R.; Guo, X.; Zhu, Y.; Cheng, W.; Li, W.; Yang, X.; Chen, H.C. Potentiostatic deposition of cobalt nickel selenides on FTO for advanced dye-sensitized solar cells. *Sol. Energy* **2019**, *179*, 59–66. [[CrossRef](#)]
22. Yeh, M.H.; Lin, L.U.; Lee, C.P.; Wei, H.Y. A composite catalytic film of PEDOT:PSS/TiN-NPs on a flexible counter-electrode substrate for a dye-sensitized solar cell. *J. Mater. Chem.* **2011**, *21*, 19021–19029. [[CrossRef](#)]
23. Li, C.T.; Lee, C.P.; Li, Y.Y.; Yeh, M.H.; Ho, K.C. SrTiCo₃ Og NPs/PEDOT-PSS counter electrodes for high efficiency dye: Sensitized solar cells. *J. Mater. Chem.* **2013**, *1*, 14888–14896. [[CrossRef](#)]
24. Wei, W.; Wang, H.; Hu, Y.H. A review on PEDOT-based counter electrodes for dye-sensitized solar cells. *Int. J. Energy Res.* **2014**, *38*, 1099–1111. [[CrossRef](#)]
25. Jing, M.; Sing, Q.; Zhang, F.; Wu, M. Improvement on the catalytic activity of the flexible PEDOT counter electrode in dye-sensitized solar cells. *Mater. Res. Bull.* **2018**, *100*, 213–219.
26. Bella, F.; Porcarelli, L.; Mantione, D.; Gerbaldi, C.; Barolo, C.; Grätzel, M.; Mecerreyes, D. A water-based and metal-free dye solar cell exceeding 7% efficiency using a cationic poly(3,4-ethylenedioxythiophene) derivative. *Chem. Sci.* **2020**, *11*, 1485–1493. [[CrossRef](#)]
27. Eliaz, N.; Venkatakrishna, K.; Hegde, A.C. Electroplating and characterization of Zn–Ni, Zn–Co and Zn–Ni–Co alloys. *Surf. Coat. Technol.* **2010**, *205*, 1969–1978. [[CrossRef](#)]
28. Lin, J.Y.; Liao, J.H.; Chou, S.W. Cathodic electrodeposition of highly porous cobalt sulfide counter electrodes for dye-sensitized solar cells. *Electrochim. Acta* **2011**, *56*, 8818–8826. [[CrossRef](#)]
29. Chae, S.Y.; Hwang, Y.J.; Choi, J.H.; Joo, O.S. Cobalt sulfide thin films for counter electrodes of dye-sensitized solar cells with cobalt complex based electrolytes. *Electrochim. Acta* **2013**, *114*, 745–749. [[CrossRef](#)]
30. Rao, S.S.; Gopi, C.V.V.M.; Kim, S.K.; Son, M.K.; Jeong, M.S.; Savariraj, A.D.; Prabakar, K.; Kim, H.J. Cobalt sulfide thin film as an efficient counter electrode for dye-sensitized solar cells. *Electrochim. Acta.* **2014**, *133*, 174–179.

31. Banerjee, A.; Upadhyay, K.K.; Bhatnagar, S.; Tathavadekar, M.; Bansode, U.; Agarkar, S.; Ogale, S.B. Nickel cobalt sulfide nanoneedle array as an effective alternative to Pt as a counter electrode in dye sensitized solar cells. *RSC Adv.* **2014**, *4*, 8289–8294. [[CrossRef](#)]
32. Duan, X.L.; Gao, Z.Y.; Changa, J.L.; Wu, D.P.; Ma, P.F.; Hea, J.J.; Xu, F.; Gao, S.; Jiang, K. CoS₂–graphene composite as efficient catalytic counter electrode for dye-sensitized solar cell. *Electrochim. Acta* **2013**, *114*, 173–179. [[CrossRef](#)]
33. Kung, C.W.; Chen, H.W.; Lin, C.Y.; Huang, K.C.; Vittal, R.; Ho, K.C. CoS Acicular Nanorod Arrays for the Counter Electrode of an Efficient Dye-Sensitized Solar Cell. *ACS Nano* **2012**, *6*, 7016–7025. [[CrossRef](#)] [[PubMed](#)]
34. Hsu, S.H.; Li, C.T.; Chien, H.T.; Salunkhe, R.R.; Suzuki, N.; Yamauchi, Y.; Ho, K.C. Platinum-Free Counter Electrode Comprised of Metal-Organic-Framework (MOF)-Derived Cobalt Sulfide Nanoparticles for Efficient Dye-Sensitized Solar Cells (DSSCs). *Sci. Rep.* **2014**, *4*, 6983. [[CrossRef](#)] [[PubMed](#)]
35. Kim, H.J.; Kim, C.W.; Punnoose, D.; Gopi, C.V.V.M.; Kim, S.K.; Prabakar, K.; SrinivasaRao, S. Nickel doped cobalt sulfide as a high performance counter electrode for dye-sensitized solar cells. *Appl. Surf. Sci.* **2015**, *328*, 78–85. [[CrossRef](#)]
36. Miao, X.H.; Pan, K.; Wang, G.F.; Liao, Y.P.; Wang, L.; Zhou, W.; Jiang, B.; Pan, Q.; Tian, G. Well-Dispersed CoS Nanoparticles on a Functionalized Graphene Nanosheet Surface: A Counter Electrode of Dye-Sensitized Solar Cells. *Chem. Eur. J.* **2014**, *20*, 474–482. [[CrossRef](#)]
37. Swami, S.K.; Chaturvedi, N.; Kumar, A.; Kapoor, R.; Dutta, V.; Frey, J.; Moehl, T.; Grätzel, M.; Mathew, S.; Nazeeruddin, M.K. Investigation of electrodeposited cobalt sulphide counter electrodes and their application in next-generation dye sensitized solar cells featuring organic dyes and cobalt-based redox electrolytes. *J. Power Sources* **2015**, *275*, 80–89. [[CrossRef](#)]
38. Mba, M.; D'Acunzo, M.; Salice, P.; Carofiglio, T.; Maggini, M.; Bignozzi, C.A. Sensitization of Nanocrystalline TiO₂ with Multibranched Organic Dyes and Co(III)/(II) Mediators: Strategies to Improve Charge Collection Efficiency. *J. Phys. Chem. C* **2013**, *117*, 19885–19896. [[CrossRef](#)]
39. Huo, J.; Zheng, M.; Tu, Y.; Wu, J.H.; Hu, L.H.; Dai, S.Y. A high performance cobalt sulfide counter electrode for dye-sensitized solar cells. *Electrochim. Acta* **2015**, *159*, 166–173. [[CrossRef](#)]
40. Wang, M.K.; Anghel, A.M.; Marsan, B.; Ha, N.L.C.; Pootrakulchote, N.; Zakeeruddin, S.M.; Grätzel, M. CoS Supersedes Pt as Efficient Electrocatalyst for Triiodide Reduction in Dye-Sensitized Solar Cells. *J. Am. Chem. Soc.* **2009**, *131*, 15976–15977. [[CrossRef](#)]
41. Sharma, J.K.; Srivastava, P.; Singh, G.; Akhtar, S.M.; Ameenc, S. Green synthesis of Co₃O₄ nanoparticles and their applications in thermal decomposition of ammonium perchlorate and dye-sensitized solar cells. *Mater. Sci. Eng. B* **2015**, *193*, 181–188. [[CrossRef](#)]
42. He, B.L.; Tang, Q.W.; Meng, X.; Yu, L.M. Poly(vinylidene fluoride)-implanted cobalt–platinum alloy counter electrodes for dye-sensitized solar cells. *Electrochim. Acta* **2014**, *147*, 209–215. [[CrossRef](#)]
43. Motlak, M.; Barakat, N.A.M.; Akhtar, M.S.; Hamza, A.H.; Kim, B.S.; Kim, C.S.; Khalil, A.K.; Almajid, A.A. High performance of NiCo nanoparticles-doped carbon nanofibers as counter electrode for dye-sensitized solar cells. *Electrochim. Acta* **2015**, *160*, 1–6. [[CrossRef](#)]
44. Zhou, S.; Jiang, Q.; Yang, J.; Chu, W.; Li, W.; Li, X.; Hou, Y.; Hou, J. Regulation of Microstructure and Composition of Cobalt Selenide Counter Electrode by Electrochemical Atomic Layer Deposition for High Performance Dye-Sensitized Solar Cells. *Electrochim. Acta* **2016**, *220*, 169–175. [[CrossRef](#)]
45. Huang, Y.J.; Lee, C.P.; Pang, H.W.; Li, C.T.; Fan, M.S.; Vittal, R.; Ho, K.C. Microemulsion-controlled synthesis of CoSe₂/CoSeO₃ composite crystals for electrocatalysis in dye-sensitized solar cells. *Mater. Today Energy* **2017**, *6*, 189–197. [[CrossRef](#)]
46. Zhao, Y.; Duan, J.; Duan, Y.; Yuan, H.; Tang, Q. 9.07%-Efficiency dye-sensitized solar cell from Pt-free RuCoSe ternary alloy counter electrode. *Mater. Lett.* **2018**, *218*, 76–79. [[CrossRef](#)]
47. Murugadoss, V.; Panneerselvam, P.; Yan, C.; Guo, Z.; Angaiah, S. A simple one-step hydrothermal synthesis of cobaltnickel selenide/graphene nanohybrid as an advanced platinum free counter electrode for dye sensitized solar cell. *Electrochim. Acta* **2019**, *312*, 157–167. [[CrossRef](#)]
48. Pang, B.; Lin, S.; Shi, Y.; Wang, Y.; Chen, Y.; Ma, S.; Feng, J.; Zhang, C.; Yu, L.; Dong, L. Synthesis of CoFe₂O₄/graphene composite as a novel counter electrode for high performance dye-sensitized solar cells. *Electrochim. Acta* **2019**, *297*, 70–76. [[CrossRef](#)]
49. Acciari, G.; Adamo, G.; Ala, G.; Busacca, A.; Caruso, M.; Giglia, G.; Imburgia, A.; Livreri, P.; Miceli, R.; Parisi, A.; et al. Experimental Investigation on the Performances of Innovative PV Vertical Structures. *Photonics* **2019**, *6*, 86. [[CrossRef](#)]